International Journal of Biological Macromolecules 182 (2021) 1331–1338

Contents lists available at ScienceDirect

International Journal of Biological Macromolecules

journal homepage: http://www.elsevier.com/locate/ijbiomac

Evaluation of bioactive release kinetics from crosslinked chitosan films with *Aloe vera*

Iratxe Zarandona [a], Nguyen Cong Minh [c], Trang Si Trung [c], Koro de la Caba [a,b,*], Pedro Guerrero [a,b]

[a] BIOMAT Research Group, University of the Basque Country (UPV/EHU), Escuela de Ingeniería de Gipuzkoa, Plaza de Europa 1, 20018 Donostia-San Sebastián, Spain
[b] BCMaterials, Basque Center for Materials, Applications and Nanostructures, UPV/EHU Science Park, 48940 Leioa, Spain
[c] Faculty of Food Technology, Nha Trang University, 02 Nguyen Dinh Chieu Street, Nha Trang City 650000, Viet Nam

ARTICLE INFO

Article history:
Received 28 February 2021
Received in revised form 5 May 2021
Accepted 12 May 2021Available online 14 May 2021

Keywords:
Chitosan
Crosslinking
Bioactive release kinetics

ABSTRACT

Thermocompression was employed to prepare citric acid-crosslinked chitosan films with *Aloe vera* (AV) as bioactive compound. Films were easy to handle and mechanical properties did not change with the addition of AV up to 10 wt%, although both TS and EAB decreased for the films with 15 wt% AV, indicating that high AV contents would hinder intermolecular interactions among the formulation components. Maillard reaction occurred between chitosan and citric acid at the processing temperature used (115 °C), while physical interactions took place with AV, as shown by FTIR analysis. All films were insoluble but displayed hydration and limited swelling due to both physical and chemical interactions promoted by AV and citric acid, respectively. A slow AV release, governed by a Fickian diffusion controlled mechanism, and an increase of surface hydrophilicity, which favors cell adhesion, were observed.

1. Introduction

Biomaterials based on biopolymers, such as chitosan, are gaining attention since their degradation products are not immunogenic [1,2]. Chitosan is a polysaccharide obtained by partial deacetylation of chitin found in crustaceans' shells, insects' exoskeletons or in fungi [3]. Due to its biological and chemical properties, such as biodegradability, biocompatibility, bioavailability, antimicrobial activity and non-toxicity [4,5] and its capability to promote tissue regeneration and prevent the formation of scar tissue, chitosan is considered a potential material for the development of biocompatible and antibacterial wound dressings [6,7]. Chitosan has been reported for various pharmacological properties and its role in tissue engineering and regenerative medicine is well documented. In this regard, the materials utilized for tissue engineering require certain biological and mechanical properties, similar to the natural extracellular matrix (ECM), for their functioning. Chitosan based structures, due to their structural similarity with glycosaminoglycans in the ECM and the ability to be molded into films, provide alternatives for tissue engineering applications and dressing materials.

In this context, films, hydrogels and nanofibers mates are the most common formats for wound dressing [8]. In particular, chitosan films are widely processed by solution casting [9]. Chitosan is soluble in aqueous solvents under acidic conditions, due to the protonation of amino groups, and the film is formed after solvent evaporation. Additionally, thermocompression is another suitable option due to its simplicity and high productivity and capacity to produce films at industrial scale [10]. The conditions employed in the above-mentioned processes, such as pH, temperature, and pressure, influences the final material properties [11]. Furthermore, the addition of a crosslinking agent helps to enhance functional properties. In this sense, citric acid can be added to react with amine and hydroxyl groups of chitosan and enhance the mechanical properties and water resistance of the resulting films [12,13]. To the best of our knowledge, few studies have reported chitosan films processed by thermocompression. Among them, Galvis-Sánchez et al. [14] prepared chitosan films with four natural deep eutectic solvents as plasticizers, and Matet et al. [15] used acetic acid as crosslinker, while Guerrero et al. [16] used citric acid. Concerning bioactives for wound dressing applications, *Aloe vera* (AV) is a perennial herb containing over 75 active ingredients, such as phenolics, sugars, amino acids, saponins and minerals [17]. Due to its physiologically active components, it has antioxidant, anti-inflammatory and antibacterial properties, which promote tissue regeneration and growth [13,17]. Additionally, *in vivo* studies showed that collagen/chitosan-glucan complex hollow fibers with AV enhanced wound closure after one week of treatment [18].

In this context, the aim of this study was to prepare chitosan films by thermocompression, using citric acid as crosslinker and *Aloe vera* as bioactive. The effect of AV concentration on the structure and thermal and

* Corresponding author at: BIOMAT Research Group, University of the Basque Country (UPV/EHU), Escuela de Ingeniería de Gipuzkoa, Plaza de Europa 1, 20018 Donostia-San Sebastián, Spain.
E-mail addresses: koro.delacaba@ehu.es (K. de la Caba), pedromanuel.guerrero@ehu.es (P. Guerrero).

https://doi.org/10.1016/j.ijbiomac.2021.05.087

physicochemical properties of the films was assessed as well as the bioactive release.

2. Materials and methods

2.1. Materials

Chitosan was extracted from shrimp shells in Nha Trang University, Vietnam. H_2O_2, NaOH, acetic acid, anhydrous citric acid and glycerol (with a purity of 99.01%) were supplied by Panreac (Barcelona, Spain). *Aloe vera* (AV) powder was supplied by Agora Valencia SL (Valencia, Spain).

2.2. Extraction and characterization of chitosan

Chitosan was obtained according to Minh et al. [19] with some modification. Chitosan was ground (100 mesh) and then soaked in NaOH solution (0.6 wt%) for 14 h at room temperature. Subsequently, H_2O_2 solution (0.6 wt%) was added and kept for 18 h at room temperature. Finally, the solid chitosan product was collected on filter cloth, washed by distilled water to neutral pH, and dried at 60 °C for 12 h.

The ash content in chitosan was determined by burning the samples at 600 °C in a muffle furnace. Additionally, protein content was measured by using the standard micro-Biuret protein assay using bovine serum albumin standards. Furthermore, the average molecular weight (M) of chitosan was determined according to a previous study [20]. Typically, 100 mg of chitosan was dissolved completely in a mixture of 0.1 M acetic acid and 0.2 M NaCl solution. The intrinsic viscosity [μ] of chitosan was determined by an Ubbelohde viscometer at 25 °C, and M of chitosan was calculated according to the Mark–Houwink equation:

$$[\mu] = K{*}M^a \tag{1}$$

where K is 1.81×10^{-3} and a is 0.93.

The degree of deacetylation (DD) of chitosan was determined based on a previous work [21]. Typically, 100 mg of chitosan were dissolved in 20 mL of 85% H_3PO_4 solution at 60 °C for 40 min. Then, 1 mL of the above solution was diluted in deionized water and kept at 60 °C for 2 h. After being cooled down to room temperature, samples were measured by UV spectroscopy at 210 nm. DD was calculated according to the following equation:

$$DD = 100{*}\left[1 - \frac{Glc\ NAc}{Glc\ NAc + GlcN}\right] \tag{2}$$

where GlcNAc refers to *N*-acetyl glucosamine and GlcN to glucosamine.

2.3. Film preparation

Compression molded chitosan films were prepared as described in a previous work [16] with some modifications. 3 g of chitosan were weighed and mixed with 20 wt% citric acid (based on chitosan weight) and 0, 5, 10, or 15 wt% AV (based on chitosan weight). In order to facilitate mixture flowing during the compression process, 9 mL of deionized water were added and, finally, 15 wt% glycerol (based on chitosan weight) was added as plasticizer. All reagents were manually mixed and stored in a plastic bag during 24 h at room temperature to hydrate the dough. Four film systems were analyzed: i) control film without *Aloe vera* (control), ii) chitosan film with 5 wt% *Aloe vera* (5AV), iii) chitosan film with 10 wt% *Aloe vera* (10AV), and iv) chitosan films with 15 wt% *Aloe vera* (15AV).

In order to mold the hydrated dough, the dough was placed between two aluminum plates, put into the press (Specac, Spain), previously heated up to 115 °C for 30 s, and pressed at 0.5 MPa for 2 min.

2.4. Film characterization

2.4.1. Fourier transform infrared (FTIR) spectroscopy

A Nicolet Nexus FTIR spectrometer (Thermo Fisher Scientific, Spain) with a Golden Gate ATR accessory was used to collect FTIR spectra. 32 scans with a resolution of 4 cm^{-1} were carried for each spectrum in the wavelength range between 4000 and 800 cm^{-1}.

2.4.2. Color

Color parameters of the films were measured using a CR-400 Minolta Chroma Meter (Konica Minolta, Spain) portable colorimeter. Ten samples were analyzed for each composition. CIELAB scale was used to measure color parameters: $L^* = 0$ (black) to $L^* = 100$ (white), $-a^*$ (greenness) to $+a^*$ (redness) and $-b^*$ (blueness) to $+b^*$ (yellowness). Films were placed on a white patron ($L^* = 97.39$, $a^* = 0.03$, $b^* = 1.77$) and the total color difference (ΔE^*) was calculated as:

$$\Delta E* = \sqrt{(\Delta L*)^2 + (\Delta a*)^2 + (\Delta b*)^2} \tag{3}$$

2.4.3. Water contact angle

Water contact angle (WCA) of films was measured by a Dataphysics Contact angle OCA (DataPhysics, Spain) equipment. 3 μL distilled water was dropped onto the film surface and the drop image was captured using a SCA20 software. Five replicates were carried out for each system.

2.4.4. Degradation degree

Degradation degree (DD) was calculated on samples conditioned in a climatic chamber (Angelantoni, Spain) at 25 °C and 50% relative humidity. Samples (W_0) were immersed in PBS (pH 7.4) at 37 °C for 2 and 7 days (W_d). Samples were dried with paper and conditioned in the climatic chamber at 25 °C and 50% RH until after reaching a constant weight. The results were taken in triplicate for each system and were calculated as follows:

$$DD(\%) = \frac{W_0 - W_d}{W_0} {*} 100 \tag{4}$$

2.4.5. Swelling measurements

Swelling test was carried out by gravimetric method. Samples of each system were immersed into 80 mL of PBS (pH 7.4) and weighed before (W_0) and after immersion (W_h) every 30 min for the first 3 h. Thereafter, measurements were carried out at 24 h and 48 h. Three replicates were taken for each system and swelling degree (S) was calculated by the following equation:

$$S\ (\%) = \frac{W_h - W_0}{W_0} {*} 100 \tag{5}$$

2.4.6. Aloe vera release

AV powder was dissolved in PBS (pH 7.4) at 37 °C. The absorbance of AV solution as a blank solution was read by a UV-VIS Multiskan SkyHigh (Thermo Fisher, Spain) spectrophotometer at 255 nm. The ratio of the AV release was determined by the calibration curve from 10 to 1000 ppm (μg/mL), and the theoretical total release was calculated from the determination of the accumulative release percentage. In order to determine AV release, film pieces (1 cm × 2 cm) were immersed into 10 mL of PBS (pH 7.4) at 37 °C for 9 days. Aliquots (2 μl) were collected at different times (1 h, 24 h, 3 d, 7 d and 9 d) and replaced with an equal volume of fresh PBS. Results were taken in triplicate for each system.

In order to analyze the mechanism of the *Aloe vera* release, Korsmeyer-Peppas model was used, since this model is the most

comprehensive semi-empirical equation to study the release from a polymeric matrix [22]:

$$M_t/M_\infty = k*t^n \quad (6)$$

where M_t/M_∞ is the ratio of AV released at time t, k is the release velocity constant and n is the release diffusion coefficient, related to the AV release mechanism.

2.4.7. Thermo-gravimetric analysis (TGA)

A Mettler Toledo TGA/SDTA 851 thermo-balance was used to measure the thermal stability of the samples. Dynamic scans from 25 to 900 °C were carried out at a constant rate of 10 °C/min under nitrogen atmosphere to avoid thermo-oxidative reactions.

2.4.8. Differential scanning calorimetry (DSC)

A Mettler Toledo DSC 822 was used to perform differential scanning calorimetry. Samples of around 3 mg were heated from −50 °C to 300 °C at a heating rate of 10 °C/min under nitrogen atmosphere to avoid oxidative reactions.

2.4.9. X-ray diffraction

X-ray diffraction (XRD) analysis was carried out at 40 kV and 40 mA by means of a PANalytic Xpert Pro (PANalytical, Almelo, The Netherlands) equipment with a diffraction unit and Cu-Kα (λ = 1.5418 Å) as a radiation source. Data were collected from 2° to 40° (step size = 0.026, time per step = 118 s).

2.4.10. Scanning electron microscopy

Scanning electron microscopy (SEM) was used to visualize cross-section morphologies of the samples. For that purpose, a Hitachi S-4800 scanning electron microscope (Hitachi High-Technologies Corporation, Tokyo, Japan) was used with an acceleration voltage of 15 kV. Samples were placed in a metallic stub and coated with gold under vacuum in argon atmosphere.

2.4.11. Mechanical properties

Mechanical properties were measured with an Instron 5967 electromechanical testing system (Instron, Spain). According to ASTM D638-03, tests were carried out with a tensile load of 500 N and a crosshead rate of 1 mm/min. Films were cut with bone shape of 4.75 mm × 22.25 mm. Five samples were measured for each system. Tensile strength (TS), elongation at break (EAB) and elastic modulus (EM) were measured as follows:

$$TS\ (MPa) = \frac{F_m}{L \cdot W} \quad (7)$$

where F_m is the maximum load (N), L is the thickness of the sample (mm), and W is the width of the sample (mm).

$$EAB\ (\%) = \frac{(l_{max} - l_0)}{l_0} \cdot 100 \quad (8)$$

where l_{max} is the length at break (mm) and l_0 is the initial length (mm).

$$EM\ (MPa) = \frac{F \cdot L_0}{A \cdot \Delta L} \quad (9)$$

where F is the applied force (N), L_0 is the initial length (mm), A is the area (mm^2), and ΔL is the change in the length (mm).

2.4.12. Statistical analysis

With the purpose of determining the significant differences between measurements, analysis of variance (ANOVA) was carried out by means of SPSS software (SPSS Statictic 25.0). Tukey's multiple range test was used for multiple comparisons among different systems with a statistical significance at the $p < 0.05$ level.

3. Results and discussion

3.1. Physicochemical properties

The characteristics of chitosan are shown in Table 1. Chitosan was white in color and highly soluble in diluted acetic acid. Chitosan had high purity with a low protein content (0.4 wt%) and a low mineral content (0.36 wt%). The degree of deacetylation (88.7%) was not affected by the mild conditions used to produce chitosan. The viscosity was 92 cP.

The FTIR spectra of chitosan and AV to determine the characteristic bands of each compound are shown in Fig. 1A. The spectrum of chitosan showed some characteristic bands: a broad band between 3000 and 3600 cm^{-1}, associated to O—H and N—H vibrations; a band at 2877 cm^{-1}, associated to aliphatic C—H stretching; a band at 1648 cm^{-1}, attributed to C═O stretching; a band at 1585 cm^{-1}, associated to NH_2 bending; two bands at 1421 cm^{-1} and 1376 cm^{-1}, assigned to CH_3 deformation; and some bands in the range from 1150 to 891 cm^{-1}, corresponding to C-O-C stretching absorption of the glycosidic ring of chitosan [23,24]. Regarding *Aloe vera*, it showed a wide band between 3000 and 3600 cm^{-1}, associated to O—H vibrations of phenolic groups, particularly, to anthraquinines such as aloin [25,26]. The band at 1639 cm^{-1} is attributed to C═O stretching and the bands in the region between 1150 and 848 cm^{-1} are assigned to C-O-C and stretching vibrations related to polysaccharides and sugars present in *Aloe vera* [27,28].

In order to assess the crosslinking effect between chitosan and citric acid, the spectra of chitosan powder and chitosan film with citric acid (control) are shown in Fig. 1B. The bands related to C—O glycosydic linkage of chitosan at 1151, 1063 and 1023 cm^{-1} are presented in both spectra. New bands were detected in control films due to the reaction of carboxyl groups of citric acid with the amino groups of chitosan forming an amide linkage [29]. The largest difference between both spectra was detected in the range of 1300–1700 cm^{-1}. In the chitosan spectrum, C═O and NH_2 bands appeared at 1648 and 1585 cm^{-1}, respectively; however, when citric acid was added, NH_2 band was more pronounced and shifted to 1553 cm^{-1}, while C═O band appeared as a small shoulder. Therefore, due to the crosslinking reaction between chitosan and citric acid (Fig. 1C), the amino group of chitosan was transformed from primary to secondary amine [16].

When *Aloe vera* was added to chitosan films, bands displacements were observed (Fig. 1D): amide II band of chitosan was shifted from 1553 cm^{-1} (control film) to 1558 cm^{-1} (10AV film); the glycosydic linkage band, which appeared at 1023 cm^{-1} for control and at 993 cm^{-1} for neat AV, was displaced to 1020 cm^{-1} for 10AV films. The same band shifts were observed for 15 AV films. These band displacements indicate physical interactions between the secondary amine and glycosydic ring of chitosan and polysaccharides and sugars of *Aloe vera*.

The interactions among the components of the film led to a chromatic change when *Aloe vera* concentration increased (Table 2). Control films had a yellowish color, showed by a positive value of b* parameter, due to the occurrence of Maillard reaction at the working temperature, 115 °C [30]. When *Aloe vera* was added, film color changed to a darker yellow, supported by the increase in b* value, especially for films with 10 and 15 wt% AV. In accordance, ΔE value indicated bigger color differences, visible to the human eye, for 10AV and 15AV films. This color change can be attributed to the anthranquinones like aloin, transformed into aloe emodin during thermal processing [31]. Aloe emodin is a

Table 1
Characteristics of the chitosan extracted from shrimp shells.

Solubility (%) of 1 wt% chitosan in 1% acetic acid	99.7 ± 0.1
Minerals (%)	0.36 ± 0.02
Protein (%)	0.41 ± 0.04
Degree of deacetylation (%)	89 ± 2
Viscosity (cP)	92 ± 7
Molecular weight (kDa)	135 ± 4

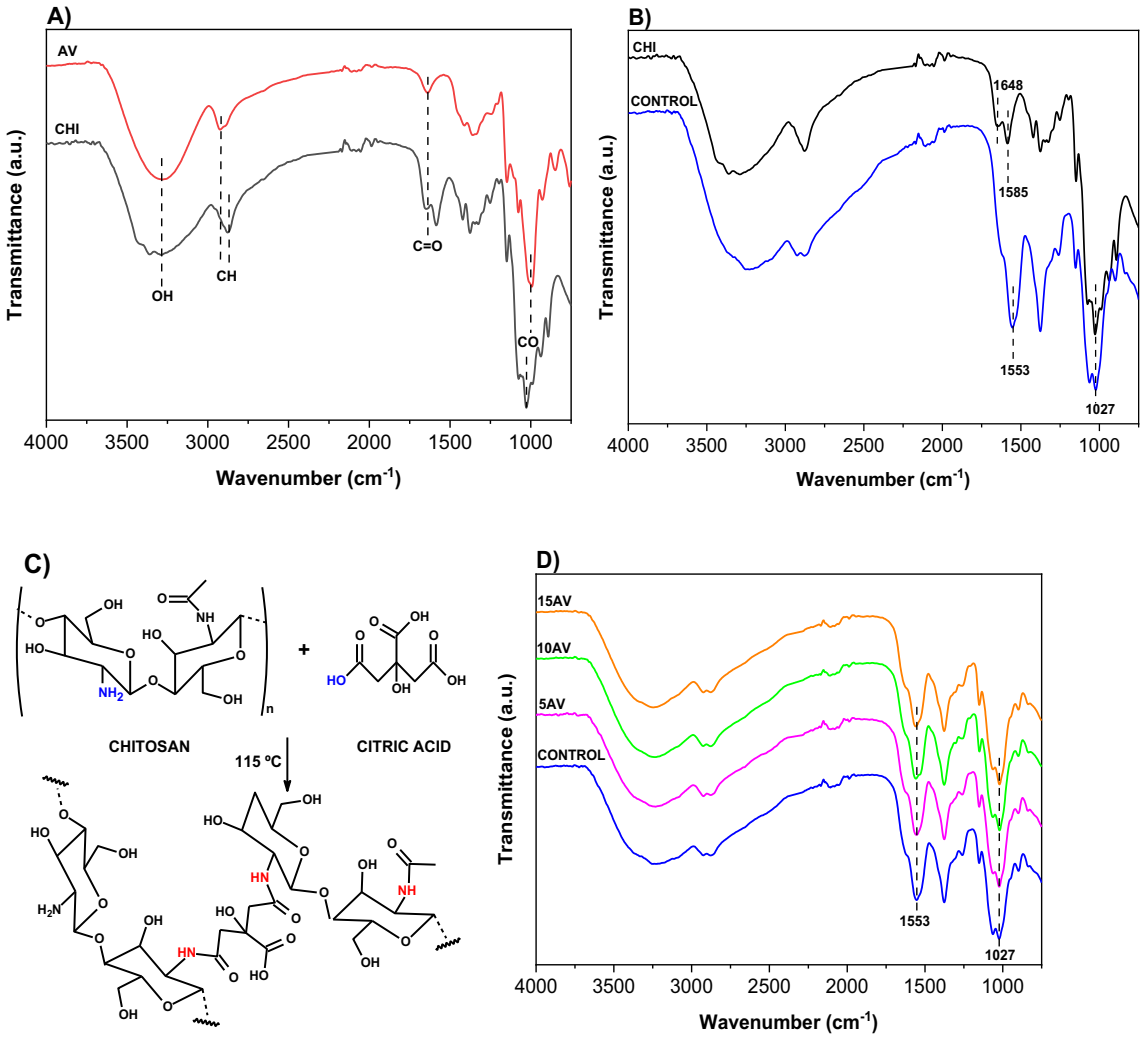

Fig. 1. FTIR spectra of A) neat chitosan (CHI) and *Aloe vera* (AV) powders. B) FTIR spectra of chitosan (CHI) powder and compression molded chitosan film (control). C) Crosslinking reaction between chitosan and citric acid. D) FTIR spectra of compression molded chitosan films without *Aloe vera* (control) and with 5 wt% *Aloe vera* (5AV), 10 wt% *Aloe vera* (10AV) and 15 wt% *Aloe vera* (15AV).

phenolic compound with anti-inflammatory, antioxidant and antibacterial activities [32].

In order to determine the effect of AV on film surface hydrophobicity or hydrophilicity, water contact angle (WCA) was measured and results are presented in Table 3. Control film showed a WCA of 83°, indicative of the film surface hydrophobicity. However, a significant decrease ($p < 0.05$) was observed when *Aloe vera* concentration increased, reaching values of 68° for 15AV films. Since many of the components of *Aloe vera* have hydrophilic character and show outstanding therapeutic activity, WCA results suggested that these polar groups of *Aloe vera* were oriented towards the film surface.

Regarding hydrolytic degradation, the values after 2 and 7 days immersed in PBS at 37 °C are shown in Table 3. At day 2, a HD value between 21 and 22% was achieved for all films, with no significant differences ($p > 0.05$) among samples. These values could be related to the glycerol migration, which is crosslinked by hydrogen bonding with chitosan and *Aloe vera*, while chemical crosslinking provides polymeric networks with resistance to degradation. After 7 days, HD was between 21 and 23%, indicating that films maintained their integrity and the crosslinking among the components of the films was successful. Additionally, there was a significant increase ($p < 0.05$) of mass loss for

Table 2
L*, a*, b* and ΔE color parameters of compression molded chitosan films without *Aloe vera* (control) and with 5 wt% *Aloe vera* (5AV), 10 wt% *Aloe vera* (10AV), and 15 wt% *Aloe vera* (15AV).

	L*	a*	b*	ΔE
Control	92.7 ± 0.3^{a}	-1.68 ± 0.05^{a}	13.4 ± 1.1^{a}	–
5AV	92.6 ± 0.3^{b}	-1.51 ± 0.05^{a}	14.9 ± 0.9^{a}	1.54
10AV	92.4 ± 0.2^{a}	-1.51 ± 0.19^{a}	19.1 ± 2.8^{b}	5.71
15AV	92.2 ± 0.5^{a}	-1.31 ± 0.06^{b}	18.9 ± 1.1^{b}	5.51

[a–b]Two means followed by the same letter in the same column are not significantly ($p > 0.05$) different according to the Tukey's multiple range test.

Table 3
Water contact angle (WCA) and hydrolytic degradation (HD) of compression molded chitosan films without *Aloe vera* (control) and with 5 wt% *Aloe vera* (5AV), 10 wt% *Aloe vera* (10AV), and 15 wt% *Aloe vera* (15AV).

Film	WCA (°)	HD (%)	
		Day 2	Day 7
Control	83 ± 1^{a}	21.2 ± 0.9^{a}	21.2 ± 0.3^{a}
5AV	78 ± 1^{b}	21.5 ± 0.5^{a}	21.7 ± 0.2^{a}
10AV	75 ± 3^{b}	22.2 ± 0.3^{a}	23.1 ± 0.2^{b}
15AV	68 ± 2^{c}	22.3 ± 0.2^{a}	23.4 ± 0.3^{b}

[a–c]Two means followed by the same letter in the same column are not significantly ($p > 0.05$) different according to the Tukey's multiple range test.

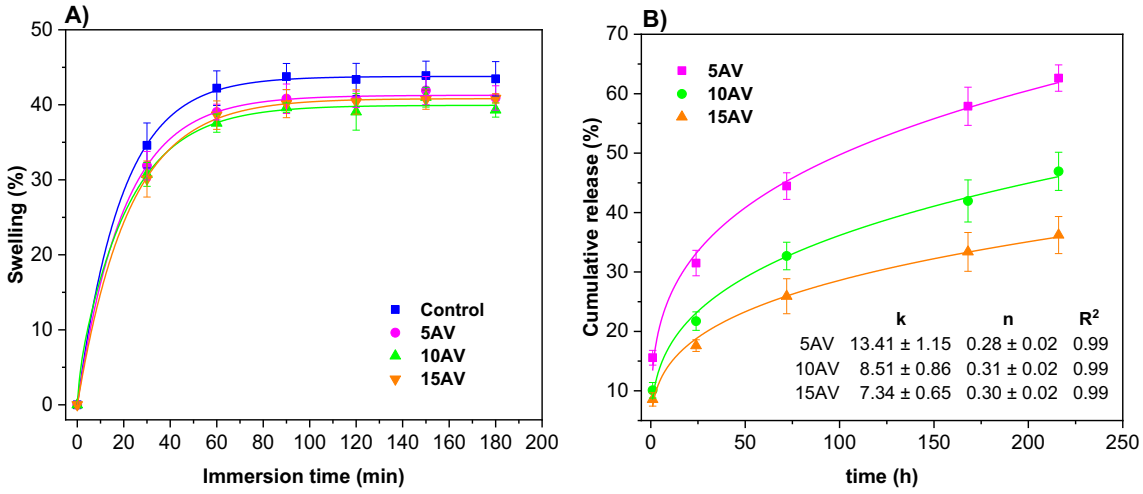

Fig. 2. A) Swelling curves and B) release of *Aloe vera* from compressed molded chitosan films without *Aloe vera* (control) and with 5 wt% *Aloe vera* (5AV), 10 wt% *Aloe vera* (10AV) and 15 wt % *Aloe vera* (15AV).

10AV and 15AV films, which can be attributed to the release of non-crosslinked *Aloe vera* at high concentrations.

Also swelling tests were performed and results are shown in Fig. 2A. It is worth noting that all samples kept their structure after 3000 min of immersion in PBS at 37 °C. In the first 30 min, swelling increased fast up to 33%. After 60 min, swelling reached the equilibrium with values of 40%, indicating that a compact structure was formed due to the interactions among the film components, which reduced the free hydrophilic moieties, preventing the absorption of large amounts of water [33]. The swelling capacity decreased when AV was added; however, no relevant differences among the films with AV were observed. This would indicate that the reaction between chitosan and citric acid would lead to a more compact network, hindering the swelling capacity of the films. It is worth noting that all films were insoluble in an aqueous environment, but displayed hydration and limited swelling. These characteristics are possible due to the presence of both physical and chemical crosslinks in the network formed. The release kinetics of bioactive compounds from a polymeric matrix is mainly dictated by the physicochemical properties of the system and the interactions between polymer, solvent and the bioactive agent. Crosslinked polymers make the penetration of water more difficult and, thus, these materials become useful for the sustained release of bioactive compounds. Therefore, controlling the rate of water diffusion is an effective strategy to control the release of the bioactive compound. Considering hydrophilic matrices with limited swelling, the mechanism of the bioactive release is controlled by the penetration velocity of the dissolution medium. When the bioactive compound is in contact with biological fluids, eventual dissolution of a small fraction of the active agent can occur, followed by hydration and progressive gelling of macromolecules, forming a high viscosity layer that increases in thickness with time. This gelled layer controls the penetration of water and constitutes a barrier to prevent the fast release of the active agent by diffusion.

The release of *Aloe vera* from chitosan films was analyzed in PBS media at 37 °C and the cumulative release during 9 days is presented in Fig. 2B. As can be seen, the release of *Aloe vera* was slow, since 63, 47 and 36% of *Aloe vera* was released from 5AV, 10AV and 15AV, respectively, at the end of the experiment (9 days). Therefore, a more sustained release of AV occurred with the increase of AV content. These results are in accordance with the physical interactions of AV with the amine groups of chitosan, as corroborated by phenolic –OH stretching in FTIR spectra, which would hinder the release of AV molecules. Moreover, the chemical reaction between chitosan and citric acid led to a more compact network, preventing a high swelling due to steric hindering and diminishing the interaction with AV. Therefore, *Aloe vera* release is governed by swelling and interactions between the components of the film forming formulation.

Cumulative release profiles give valuable information and indication about the release kinetics and mechanisms. In order to assess the

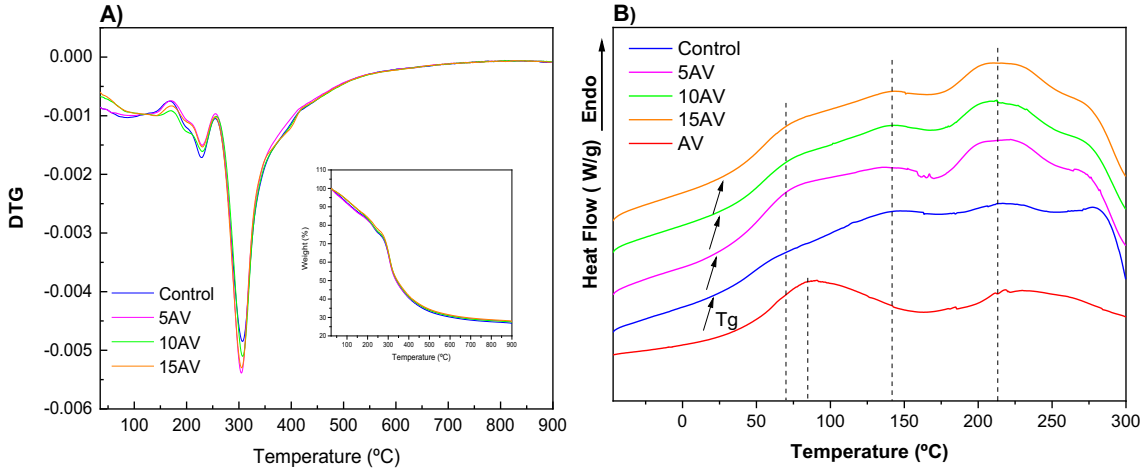

Fig. 3. A) Thermo-gravimetric analysis (TGA) curves (inset) and derivative thermo-gravimetric (DTG) curves and B) Differential scanning calorimetry (DSC) analysis of *Aloe vera* (AV) and compression molded chitosan films without *Aloe vera* (control) and with 5 wt% *Aloe vera* (5AV), 10 wt% *Aloe vera* (10AV) and 15 wt% *Aloe vera* (15AV).

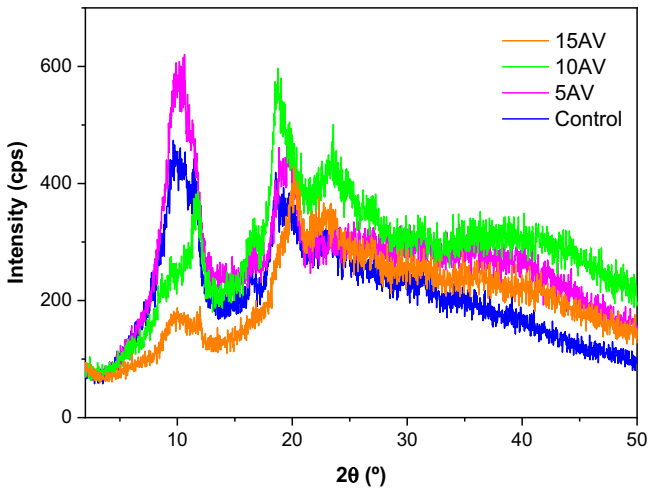

Fig. 4. Diffractograms of compressed molded chitosan films without *Aloe vera* (control), 5% *Aloe vera* (5AV), 10% *Aloe vera* (10AV) and 15% *Aloe vera* (15AV).

release mechanism, Korsmeyer-Peppas model was considered. Results were fitted to the semi-empirical equation of Korsmeyer-Peppas model, which stablishes an exponential relationship between time and release (Fig. 2B) with correlation coefficients (R^2) of 0.99 for all the systems analyzed. The diffusion exponent in the Korsmeyer-Peppas model (n) can change depending on the release main mechanism: $n < 0.5$ indicates a diffusion controlled (Fickian) release mechanism, $0.5 < n < 1$ indicates a non-Fickian diffusion and erosion release mechanism, and $n > 1$ indicates a non-Fickian erosion controlled release mechanism [34]. Considering that n values shown in Fig. 2B inset are 0.28, 0.31 and 0.30 for 5AV, 10AV and 15AV films, respectively, all films presented a Fickian diffusion controlled release mechanism, in which swelling and relaxation of chitosan chains were involved [35]. It is worth noting that the low swelling degree of the films, shown in Fig. 2A, led to a sustained release. Furthermore, these results are in agreement with those studies that indicate that release at temperatures higher than the T_g of the material are associated to the Fickian diffusion mechanism, while release at temperatures close to or slightly lower than T_g shows non-Fickian diffusion [36].

3.2. Thermal properties

Thermo-gravimetric analysis (TGA) and differential scanning calorimetry (DSC) were carried out in order to study the changes occurred by the temperature effect. Regarding TGA, weight loss curves and derivative thermo-gravimetric curves are presented in Fig. 3A. As can be observed, three main weight loss steps are presented. The first one, around 100 °C, can be related to the loss of moisture. In the case of 10AV and 15AV films, weight loss started at a higher temperature, around 110 °C, which can be attributed to the interactions observed by FTIR, that could form a leaner structure and, thus, more energy was needed to release water. The second step, around 228 °C, can be attributed to the evaporation of glycerol [30] and to the thermal depolymerization of *Aloe vera*'s hemicellulose, lignin and cellulose [37]. The third step, the main mass loss, occurred around 304 °C and can be assigned to the chitosan degradation step [38] and to the degradation of α-cellulose present in *Aloe vera* [37].

Concerning DSC analysis, results are shown in Fig. 3B. *Aloe vera* sample showed two endothermic peaks: at 91 °C, related to the sample moisture, and at 218 °C, associated to the water entangled into the *Aloe vera* components [39]. Films presented three endothermic peaks: the first peak at 74 °C can be related to film moisture; the second peak at 141 °C corresponding to the entrapped water linked to the film components by hydrogen bonding, since a tighter structure was formed and more energy was needed to release water; the last peak at 209 °C was

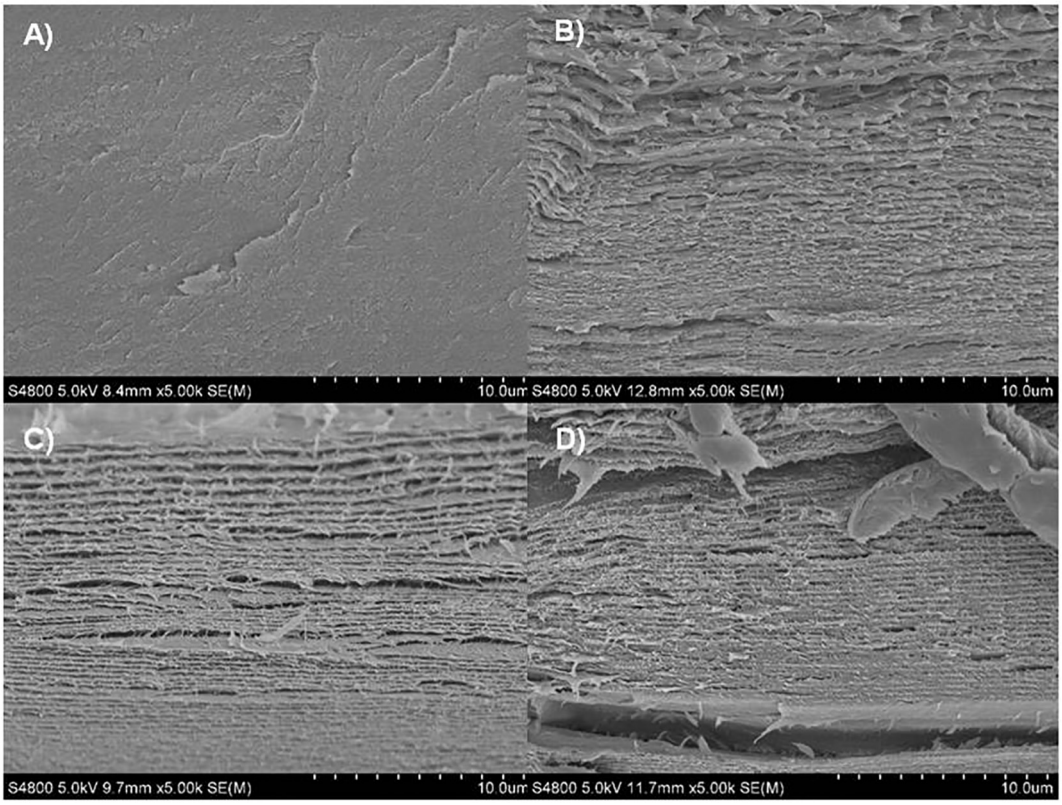

Fig. 5. SEM images of cross-sections of compressed molded chitosan films: A) without *Aloe vera* and with B) 5% *Aloe vera* (5AV), C) 10% *Aloe vera* (10AV), and D) 15% *Aloe vera* (15AV).

associated to the melting point of citric acid and to the hemicellulose, lignin and cellulose present in *Aloe vera*, since this peak is more pronounced for the films containing *Aloe vera* than for control films. It is worth noting that the displacement of the melting point of citric acid from since 153 (neat citric acid) to 209 °C indicated that citric acid was crosslinked to chitosan. Furthermore, glass transition temperature (T_g) increased from 21 °C (control) to 27 °C (15AV), indicating that the material stiffness increased [40]. Likewise, it can be assumed that *Aloe vera* interacted with the other components of the film.

3.3. Film structure and mechanical properties

In order to study the influence of *Aloe vera* in the structure of compressed molded chitosan films, XRD analysis was performed and XRD patterns are shown in Fig. 4. Control films showed two broad diffraction peaks at around $2\theta = 10.5°$ and 19°, corresponding to the characteristics peaks of chitosan [41,42]. When *Aloe vera* concentration was increased, the intensity of the diffraction peaks decreased. The interactions between chitosan and *Aloe vera* could difficult the mobility of chitosan chains and, thus, hindered the crystallization process.

In agreement to XRD results, SEM images (Fig. 5) showed cross-section images of chitosan films. As can be seen, a compact structure was observed in control films, indicating a good compatibility between the components of the films. When *Aloe vera* was added, a structure formed by overlapping layers was observed, suggesting that film structure changed by the interactions of *Aloe vera* with the components of the films, as shown by FTIR analysis.

Regarding mechanical properties, tensile strength (TS), elongation at break (EAB), and elastic modulus (EM) are shown in Table 4 in order to assess the effect of AV content in the mechanical behavior of chitosan films. No significant differences ($p > 0.05$) were observed in EAB, TS, or E values when *Aloe vera* was added up to 10 wt%. However, EAB and TS values showed a decrease for 15AV films. These results would indicate the hindrance effect of *Aloe vera* at high concentration (15AV film), avoiding intermolecular interactions between the components of the film forming formulations and, thus, decreasing TS values [43,44]. Moreover, the decrease of EAB when *Aloe vera* content increased was related to the lack of plasticizing effect of *Aloe vera* [44]. As shown by previous analyses, mechanical properties also showed that the highest AV content under study did not lead to improvements.

4. Conclusions

Chitosan films with *Aloe vera* were successfully processed by thermocompression. The crosslinking reaction between the amino group of chitosan and the carboxyl groups of citric acid was confirmed by FTIR analysis. It is worth noting that crosslinked chitosan films maintained their integrity after 9 days in PBS at 37 °C. In addition, the formed structure was compact, limiting the swelling capacity of the films. In this regard, films presented a Fickian diffusion controlled release mechanism, in which swelling and relaxation of chitosan chains were involved, leading to a sustained release of *Aloe vera*. Although further assessments are required, this work showed the potential of citric-acid crosslinked chitosan films for biomedical applications, such as wound healing.

Table 4
Tensile strength (TS), elongation at break (EAB) and elastic modulus (EM) of compressed molded chitosan films without *Aloe vera* and with 5% *Aloe vera* (5AV), 10% *Aloe vera* (10AV), and 15% *Aloe vera* (15AV).

Films	TS (MPa)	EAB (%)	EM (MPa)
Control	17.91 ± 0.95^{a}	15.66 ± 1.46^{a}	909.18 ± 83.55^{a}
5AV	16.20 ± 1.03^{a}	$14.93 \pm 0.51^{a,b}$	949.89 ± 66.74^{a}
10AV	15.65 ± 1.98^{a}	$13.11 \pm 2.02^{a,b}$	$857.86 \pm 54.43^{a,b}$
15AV	12.33 ± 1.74^{b}	12.60 ± 1.87^{b}	770.71 ± 58.53^{b}

[a–b]Two means followed by the same letter in the same column are not significantly ($p > 0.05$) different according to the Tukey's multiple range test.

CRediT authorship contribution statement

Conceptualization, K·C and P.G.; resources, K·C., P.G. and T.S.T.; investigation, I.Z. and N.C.M.; supervision, K·C and P.G.; writing—original draft preparation, I.Z. and N.C.M.; writing—review and editing, K·C, P.G. and T.S.T; funding acquisition, K.C and T.S.T.

Acknowledgments

This research was funded by MCIU/AEI/FEDER, UE (RTI2018-097100-B-C22). Iratxe Zarandona thanks the Quality and Food Industry Department of the Basque Government for her fellowship (22-2018-00078). Also thanks are due to the Advanced Research Facilities (SGIker) from the UPV/EHU.

References

[1] M.K. Ahmed, A.M. Moydeen, A.M. Ismail, M.E. El-Naggar, A.A. Menazea, M.H. El-Newehy, Wound dressing properties of functionalized environmentally biopolymer loaded with selenium nanoparticles, J. Mol. Struct. 1225 (2021), 129138, .
[2] R, Rebelo, M. Fernandes, R. Fangueiro, Biopolymers in medical implants: a brief review, Procedia Eng. 200 (2017) 236–243.
[3] S. Sarkar, D. Das, P. Dutta, J. Kalita, S.B. Wann, P. Manna, Chitosan: a promising therapeutic agent and effective drug delivery system in managing diabetes mellitus, Carbohyd. Polym. 247 (2020), 116594, .
[4] S.I. Ahmad, R. Ahmad, M.S. Khan, R. Kant, S. Shahid, L. Gautam, G.M. Hasan, M.-I. Hassan, Chitin and its derivatives: structural properties and biomedical applications, Int. J. Biol. Macromol. 164 (2020) 526–539.
[5] T. Takei, S. Danjo, S. Sakoguchi, S. Tanaka, T. Yoshinaga, H. Nishimata, M. Yoshida, Autoclavable physically-crosslinked chitosan cryogel as a wound dressing, J. Biosci. Bioeng. 125 (2018) 490–495.
[6] X. Sun, M. Dong, Z. Guo, H. Zhang, J. Wang, P. Jia, T. Bu, Y. Liu, L. Li, L. Wang, Multifunctional chitosan-copper-gallic acid based antibacterial nanocomposite wound dressing, Int. J. Biol. Macromol. 167 (2021) 10–22.
[7] S. Bose, C. Koski, A.A. Vu, Additive manufacturing of natural biopolymers and composites for bone tissue engineering, Mater. Horiz. 7 (2020) 2011–2027.
[8] S. Shahzad, M. Yar, S.A. Siddiqi, N. Mahmood, A. Rauf, Z.A. Qureshi, M.S. Anwar, S. Afzaal, Chitosan-based electrospun nanofibrous mats, hydrogels and cast films: novel anti-bacterial wound dressing matrices, J. Mater. Sci. Mater. Med. 26 (2015) 136.
[9] A. Muxika, A. Etxabide, J. Uranga, P. Guerrero, K. de la Caba, Chitosan as a bioactive polymer: processing, properties and applications, Int. J. Biol. Macromol. 105 (2017) 1358–1368.
[10] C. Valencia-Sullca, L. Atarés, M. Vargas, A. Chiralt, Physical and antimicrobial properties of compression-molded cassava starch-chitosan films for meat preservation, Food Bioprocess Technol. 11 (2018) 1339–1349.
[11] O. Ochoa-Yepes, L. Di Giogio, S. Goyanes, A. Mauri, L. Fama, Influence of process (extrusion/thermo-compression, casting) and lentil protein content on physicochemical properties of starch films, Carbohydr. Polym. 208 (2019) 221–231.
[12] A. Oryan, A. Kamali, A. Moshiri, H. Baharvand, H. Daemi, Chemical crosslinking of biopolymeric scaffolds: current knowledge and future directions of crosslinked engineered bone scaffolds, Int. J. Biol. Macromol. 107 (2018) 678–688.
[13] S.R. Kanatt, S.H. Makwana, Development of active, water-resistant carboxymethyl cellulose-poly vinyl alcohol-*Aloe vera* packaging film, Carbohydr. Polym. 227 (2020), 115303, .
[14] A.C. Galvis-Sánchez, A.C.R. Castro, K. Biernacki, M.P. Gonçalves, H.K.S. Souza, Natural deep eutectic solvents as green plasticizers for chitosan thermoplastic production with controlled/desired mechanical and barrier properties, Food Hydrocoll. 82 (2018) 478–489.
[15] M. Matet, M.C. Heuzey, E. Pollet, A. Ajji, L. Averous, Innovative thermoplastic chitosan obtained by thermo-mechanical mixing with polyol plasticizers, Carbohydr. Polym. 95 (2013) 241–251.
[16] P. Guerrero, A. Muxika, I. Zarandona, K. de la Caba, Crosslinking of chitosan films processed by compression molding, Carbohydr. Polym. 206 (2019) 820–826.
[17] S.M.T. Tapeh, M.S. Baei, S.H. Keshel, Synthesis of thermogel modified with biomaterials as carrier for hUSSCs differentiation into cardiac cells: physicomechanical and biological assessment, Mater. Sci. Eng. C-Mater. 119 (2021) 111517.
[18] A.M. Abdel-Mohsen, J. Frankova, R.M. Abdel-Rahman, A.A. Salem, N.M. Sahffie, I. Kubena, J. Jancar, Chitosan-glucan complex hollow fibers reinforced collagen wound dressing embedded with aloe vera. II multifunctional properties to promote cutaneous wound healing, Int. J. Pharm. 582 (2020), 119349, .
[19] N.C. Minh, N.H. Cuong, P.T.D. Phuong, S. Schwarz, W.F. Stevens, N.V. Hoa, T.S. Trung, Swelling-assisted reduction of chitosan molecular weight in the solid state using hydrogen peroxide, Polym. Bull. 74 (2017) 3077–3087.
[20] M. Rinaudo, Chitin and chitosan: properties and applications, Prog. Polym. Sci. 31 (2006) 603–632.

[21] N.C. Minh, V.H. Nguyen, S. Schwarz, W.F. Stevens, T.S. Trung, Preparation of water soluble hydrochloric chitosan from low molecular weight chitosan in the solid state, Int. J. Biol. Macromol. 121 (2019) 718–726.
[22] M.L. Bruschi, Strategies to modify the drug release from pharmaceutical systems. In M.L. Bruschi (Eds.), Mathematical Models of Drug Release, Sawston: Woodhead Publishing, 2015, pp. 63–86.
[23] H.F.G. Barbosa, D.S. Francisco, A.P.G. Ferreira, E.T.G. Cavalheiro, A new look towards the thermal decomposition of chitins and chitosans with different degrees of deacetylation by coupled TG-FTIR, Carbohydr. Polym. 225 (2019), 115232, .
[24] R.A. Mauricio-Sánchez, R. Salazar, J.G. Luna-Bárcenas, A. Mendoza-Galván, FTIR spectroscopy studies on the spontaneous neutralization of chitosan acetate films by moisture conditioning, Vib. Spectrosc. 94 (2018) 1–6.
[25] F.R. Isfahani, H. Tavanai, M. Morshed, Release of Aloe vera from electrospun Aloe vera-PVA nanofibrous pad, Fiber Polym. 18 (2017) 264–271.
[26] S. Torres-Giner, S. Wilkanowicz, B. Melendez-Rodriguez, J.M. Lagaron, Nanoencapsulation of *Aloe vera* in synthetic and naturally occurring polymers by electrohydrodynamic processing of interest in food technology and bioactive packaging, J. Agric. Food Chem. 65 (2017) 4439–4448.
[27] D. Bajer, K. Janczak, K. Bajer, Novel starch/chitosan/Aloe vera composites as promising biopackaging materials, J. Polym. Environ. 28 (2020) 1021–1039.
[28] A.K. Prajapati, S. Das, M.K. Mondal, Exhaustive studies on toxic Cr(VI) removal mechanism from aqueous solution using activated carbon of *Aloe vera* waste leaves, J. Mol. Liq. 307 (2020), 112956, .
[29] S.M. Gawish, S.M. Abo El-Ola, A.M. Ramadan, A.A. Abou El-Kheir, Citric acid used as a crosslinking agent for the grafting of chitosan onto woolen fabric, J. Appl. Polym. Sci. 123 (2012) 3345–3353.
[30] I. Leceta, P. Guerrero, I. Ibarburu, M.T. Dueñas, K. de la Caba, Characterization and antimicrobial analysis of chitosan-based films, J. Food Eng. 116 (2013) 889–899.
[31] X.L. Chang, C. Wang, Y. Feng, Z. Liu, Effects of heat treatments on the stabilities of polysaccharides substances and barbaloin in gel juice from *Aloe vera* miller, J. Food Eng. 75 (2006) 245–251.
[32] S. Rahman, P. Carter, N. Bhattarai, Aloe Vera for tissue engineering applications, J. Funct. Biomater. 8 (2017) 6.
[33] A.R. Deshmukh, H. Aloui, C. Khomlaem, A. Negi, J.H. Yun, H.S. Kim, B.S. Kim, Biodegradable films based on chitosan and defatted *Chlorella* biomass: functional and physical characterization, Food Chem. 337 (2021), 127777, .
[34] S. Tan, C. Zhong, T. Langrish, Encapsulation of caffeine in spray-dried micro-eggs for controlled release: the effect of spray-drying (cooking) temperature, Food Hydrocoll. 108 (2020), 105979, .
[35] G.B. Li, J. Wang, X.P. Kong, Coprecipitation-based synchronous pesticide encapsulation with chitosan for controlled spinosad release, Carbohydr. Polym. 249 (2020), 116865, .
[36] G.M. Gomes, J.P. Bigon, F.E. Montoro, L.M.F. Lona, Encapsulation of N,N-diethyl-*meta*-toluamide (DEET) via miniemulsion polymerization for temperature controlled releasem, J. Appl. Polym. Sci.. 136 (2019) 47139.
[37] A.N. Balaji, K.J. Nagarajan, Characterization of alkali treated and untreated new cellulosic fiberfrom Saharan aloe vera cactus leaves, Carbohydr. Polym. 174 (2017) 200–208.
[38] M. Andonegi, K. Las Heras, E. Santos-Vizcaíno, M. Igartua, R.M. Hernandez, K. de la Caba, P. Guerrero, Structure-properties relationship of chitosan/collagen films with potential for biomedical applications, Carbohydr. Polym. 237 (2020) 116159.
[39] R. Pereira, A. Tojeire, D.C. Vaz, A. Mendes, P. Bártolo, Preparation and characterization of films based on alginate and Aloe vera, Int. J. Polym. Anal. Charact. 16 (2011) 449–464.
[40] N. Dehouche, C. Idres, M. Kaci, I. Zembouai, S. Bruzaud, Effects of various surface treatments on Aloe Vera fibers used as reinforcement in poly(3-hydroxybutyrate-co-3-hydroxyhexanoate) (PHBHHx) biocomposites, Polym. Degrad. Stab. 175 (2020) 109131.
[41] M. Liu, Y. Zhou, Y. Zhang, C. Yu, S. Cao, Preparation and structural analysis of chitosan films with and without sorbitol, Food Hydrocoll.. 33 (2013) 186–191.
[42] X. Ma, C. Qiao, X. Wang, J. Yao, J. Xu, Structural characterization and properties of polyols plasticized chitosan films, Int. J. Biol. Macromol. 135 (2019) 240–245.
[43] T.J. Gutiérrez, G. González, Effect of cross-linking with *Aloe vera* gel on surface and physicochemical properties of edible films made from plantain flour, Food Biophys 12 (2017) 11–22.
[44] M.I. Pinzon, O.R. Garcia, C.C. Villa, The influence of *Aloe vera* gel incorporation on the physicochemical and mechanical properties of banana starch-chitosan edible films, J. Sci. Food Agric. 98 (2018) 4042–4049.